Theor Chem Acc (2014) 133:1429
DOI 10.1007/s00214-013-1429-6

REGULAR ARTICLE

Comparison of multireference configuration interaction potential energy surfaces for $H + O_2 \rightarrow HO_2$: the effect of internal contraction

Lawrence B. Harding · Stephen J. Klippenstein · Hans Lischka · Ron Shepard

Received: 11 September 2013 / Accepted: 20 November 2013
© Springer-Verlag Berlin Heidelberg (outside the USA) 2013

Abstract A comparison is presented of uncontracted multireference singles and doubles configuration interaction (MRCI) and internally contracted MRCI potential energy surfaces for the reaction $H(^2S) + O_2\left(^3\sum_g^-\right) \rightarrow HO_2(^2A'')$. It is found that internal contraction leads to significant differences in the reaction kinetics relative to the uncontracted calculations.

Keywords MRCI · Internal contraction · $H + O_2$

1 Introduction

The reaction of hydrogen atom with molecular oxygen

$$H(^2S) + O_2\left(^3\Sigma_g^-\right) \rightarrow HO_2(^2A'') \quad (1)$$

on the electronic ground state potential energy surface (PES) is important in both combustion and atmospheric chemistry. Several experimental [1–4] and theoretical [5–10] studies of the high-pressure limit for this reaction have been reported. All the theoretical studies are based on multireference electronic structure methods. Multireference methods are appropriate here because the reaction results in a change in the number of open-shell orbitals, three for the reactants and just one for the product. Probably the most accurate, global, HO_2 PES currently available was reported in 2005 by Xu et al. [11]. It consists of a spline fit to 15,000 internally contracted multireference configuration interaction (ic-MRCI) energies employing the Dunning, aug-cc-pVQZ basis set and the Davidson correction for higher-order excitations.

The theoretical studies reported in Refs. [5, 10] both employ MRCI calculations with the same, 7-orbital 9-electron, active space and the same orbital basis set (aug-cc-pVTZ). The only difference between the two calculations is that the earlier study is an uncontracted MRCI (uc-MRCI) calculation computed with the COLUMBUS program package [12], while the more recent study is an ic-MRCI calculation computed with the MOLPRO program package [13]. Figure 1 of Ref. [10] shows significant differences between the minimum energy path (MEP) energies from the uncontracted and internally contracted calculations. The purpose of this communication is to explore further the differences between the uc-MRCI and ic-MRCI results for this reaction, and to determine the effect these differences have on the predicted high-pressure-limit reaction rate.

The paper is organized as follows. A brief summary of the uc-MRCI and ic-MRCI methods is presented in Sect. 2. The electronic structure calculations are described in Sect. 3. The transition state theory (TST) calculations of the reaction rates are described in Sect. 4. In Sect. 5, the results of the calculations are presented and discussed. The paper concludes with Sect. 6.

Dedicated to Professor Thom Dunning and published as part of the special collection of articles celebrating his career upon his retirement.

Electronic supplementary material The online version of this article (doi:10.1007/s00214-013-1429-6) contains supplementary material, which is available to authorized users.

L. B. Harding (✉) · S. J. Klippenstein · H. Lischka · R. Shepard
Chemical Sciences and Engineering Division, Argonne National Laboratory, Argonne, IL 60439, USA
e-mail: harding@anl.gov

H. Lischka
Department of Chemistry and Biochemistry, Texas Tech University, Lubbock, TX 79409, USA

Published online: 08 December 2013

2 The uc-MRCI and ic-MRCI formalisms

In a MRCI approach, the wave function is expanded in a basis of reference functions and excitations from those reference functions. In this work, which involves open-shell molecular radical species, the expansion functions are chosen to be spin-adapted configuration state functions (CSF) rather than primitive Slater determinants.

$$|\psi^{\mathrm{MRCI}}\rangle = \sum_{n}^{N_{\mathrm{dim}}} c_n|n\rangle = \sum_{m}^{N_{\mathrm{ref}}} c(m)|m;\mathrm{ref}\rangle + \sum_{m}^{N_{\mathrm{ref}}}\sum_{pq} c(m)_q^p \left|m_q^p\right\rangle + \sum_{m}^{N_{\mathrm{ref}}}\sum_{pqrs} c(m)_{qs}^{pr}\left|m_{qs}^{pr}\right\rangle + \cdots$$

with

$$\left|m_q^p\right\rangle = E_{pq}|m;\mathrm{ref}\rangle;\left|m_{qs}^{pr}\right\rangle = e_{pqrs}|m;\mathrm{ref}\rangle;\ldots$$

E_{pq} and e_{pqrs} are the spin-adapted single- and double-excitation operators. The expansion space employed in the present calculations is limited to single and double excitations, which is typical for MRCI applications.

In general, the orbital summations range over all the molecular orbital (MO) basis functions, but when the reference functions are constructed from doubly occupied and active orbital subsets, the allowed combinations of orbital indices in the excitation operators are correspondingly restricted. Furthermore, the above basis functions are typically linearly dependent, which results in further restrictions in the summations. One type of linear dependency occurs when, for example, the molecular orbital φ_s is unoccupied in the reference function $|m;\mathrm{ref}\rangle$, in which case the basis functions $\left|m_{qs}^{pr}\right\rangle$ should be eliminated from the expansion. A second type of linear dependency occurs when the same expansion function is generated from two different reference functions, $\left|m_{qs}^{pr}\right\rangle = \left|m_{q's'}^{'p'r'}\right\rangle$, in which case only a single instance of the function should be included in the expansion.

An alternative approach to define the expansion space consists of imposing orbital occupation restrictions on subsets of the orbitals to generate the reference functions $|m;\mathrm{ref}\rangle$ along with a consistent set of orbital occupation restrictions for the single and double excitations. This occupation restriction approach eliminates the complications associated with linear dependence of the basis, but it imposes some restrictions on the general form of the expansion space, and it may also include expansion terms that do not belong to the minimal interacting space [14]. In the COLUMBUS program system, these occupation restrictions are imposed by restricting the allowed nodes of the Shavitt graph in the Graphical Unitary Group Approach (GUGA) (see ref. [12] and references therein).

In the following discussion, the above expansion basis, after the appropriate elimination of linear dependencies, will be called the uc-MRCI space. As discussed in ref. [15], the uc-MRCI expansion dimension N_{dim} increases, approximately linearly, with the reference space dimension N_{ref}, resulting in expensive computational procedures and limiting the application of the method generally with respect to molecular system size.

In order to reduce the expansion dimension and the corresponding computational costs of MRCI, the internal contraction approximation was introduced [16, 17]. In this ic-MRCI approximation, the excitation operators are applied to the contracted reference wave function rather than to the individual reference basis functions,

$$\left|\psi^{ic-\mathrm{MRCI}}\right\rangle = \sum_{n}^{N_{\mathrm{dim}}} \tilde{c}_n|\tilde{n}\rangle = \tilde{c}_0\left|\tilde{\psi}_0\right\rangle + \sum_{pq}\tilde{c}_q^p\left|\tilde{\psi}_q^p\right\rangle + \sum_{pqrs}\tilde{c}_{qs}^{pr}\left|\tilde{\psi}_{qs}^{pr}\right\rangle$$

with

$$\left|\tilde{\psi}_0\right\rangle = \sum_{m}^{N_{\mathrm{ref}}} c_m^{\mathrm{ref}}|m;\mathrm{ref}\rangle;\left|\tilde{\psi}_q^p\right\rangle = E_{pq}\left|\tilde{\psi}_0\right\rangle;\left|\tilde{\psi}_{qs}^{pr}\right\rangle = e_{pqrs}\left|\tilde{\psi}_0\right\rangle.$$

The reference expansion coefficients c_m^{ref} are typically fixed at their optimal MCSCF values and not allowed to vary during the subsequent CI optimization. Thus, the number of variational coefficients N_{dim} in ic-MRCI is comparable to that of a single-reference calculation and is reduced significantly compared to the uc-MRCI dimension. The ic-MRCI expansion spans a subspace of the minimal interacting space [17].

One of the most popular implementations of the ic-MRCI method is the MOLPRO program [13, 18–21]. In this particular implementation, only the double excitations are contracted, the reference functions and the single excitations are left uncontracted. This hybrid approach increases the flexibility of the wave function compared to the fully ic-MRCI expansion while still reducing the computational costs significantly compared to the uc-MRCI expansion.

Both the uc-MRCI and the ic-MRCI energies satisfy the variational bound properties that the computed energies are rigorous upper bounds to the full-CI energies computed with the same MO basis, provided that no further approximations to the Hamiltonian operator or to the computed integrals are imposed. The full-CI energies computed with a given MO basis in turn are upper bounds to the complete-CI energies. The complete-CI energy is the limit of a full-CI energy within a complete MO basis and is the exact solution to the Schrodinger equation within the Born–

Oppenheimer approximation. Because the ic-MRCI expansion spans a subspace of the uc-MRCI expansion, there is also a variational bound relation between these two PESs. Furthermore, these bound relations hold for arbitrary ground and excited electronic states.

$$E_k^{\text{complete}-\text{CI}} \leq E_k^{\text{full}-\text{CI}} \leq E_k^{\text{uc}-\text{MRCI}} \leq E_k^{\text{ic}-\text{MRCI}}$$

See ref. [15] for a more complete discussion of the consequences of the ic-MRCI approximation.

Many molecular properties involve energy differences rather than total energies, and in these cases it is possible for a less-flexible method to enjoy a more favorable cancelation of errors. This cancelation of error may be fortuitous, or it may be systematic. In such a situation, the accuracy of the computed properties may not agree with the above ordering of the accuracies of the total energies. The computed reaction rates discussed in the present work depend on such energy differences. These rates depend on the behavior of the PESs, in particular barrier heights and the associated reaction-path partition functions, relative to the asymptotic dissociation limits; these shifted PESs are called *interaction potentials*.

3 Electronic structure calculations

The MRCI calculations employ a 7-orbital 9-electron active space, consisting of all valence orbitals except for the oxygen 2s orbitals that correspond to low-lying lone-pair spectator orbitals for this reaction. The Dunning aug-cc-pVTZ basis set [22] is used for all atoms, resulting in 115 total MOs. Calculations were performed in the standard Jacobi coordinates, R_{OO}, R_{MH} and the HMO angle, where M is the center of mass of the O_2 fragment. The calculations were carried out on a $9 \times 31 \times 17$ grid covering ranges of 1.14–1.38 Å for R_{OO}, 1.3–8.0 Å for R_{MH} and 0°–90° for the HMO angle. The resulting grids of energies were then fit using three-dimensional splines. Both the contracted and the uncontracted calculations were corrected for higher-order excitations with two different approaches. The Davidson correction is an a posteriori correction applied to the MRCI energy, and the averaged quadratic coupled cluster [23] (AQCC) method is an a priori correction in which the CI equation itself is modified. See ref. [15] for a detailed discussion of both approaches. The uc-MRCI and uc-AQCC calculations were computed with the COLUMBUS program system [12], and the ic-MRCI and ic-AQCC calculations were computed with the MOLPRO program [13]. All calculations were performed within the C_s point group. The molecular orbitals were determined with CASSCF calculations, and the four electrons in the O atom 1 s core orbitals were frozen in the subsequent MRCI expansions.

The internal orbital space consists of the active orbitals plus the two spectator oxygen 2 s orbitals. This expansion is denoted CAS+1+2. The uc-MRCI expansions consist of 868 internal CSFs (the 240 reference CSFs of A'' symmetry plus excitations within the internal orbital space), 277,727 single excitations, and 27,836,460 double excitations, resulting in $N_{\text{dim}} = 28{,}115{,}055$ total CSFs. In the ic-MRCI calculations, the double excitations are contracted down to 225,117 expansion terms, resulting in an expansion space of dimension $N_{\text{dim}} = 503{,}712$. The ic-MRCI expansion spans a subspace of the minimal interacting space [14, 17], whereas the uc-MRCI expansion includes also terms that interact only indirectly with the references.

Finally, as an additional check on the accuracy of the MRCI calculations, full-CI calculations were carried out along a one-dimensional path. These calculations used the Dunning VDZ basis set [24] (no polarization functions) with the OO distance fixed at R_e and the HOO angle fixed at 115°. These full-CI calculations were performed with MOLPRO [13, 18, 19].

4 Transition state theory calculations

Variable reaction coordinate transition state theory (VRC-TST) [25, 26] was used to predict the $H + O_2$ high-pressure recombination rate coefficient. The calculations were performed for the four separate analytical potential energy surfaces obtained from fits to the ic-MRCI, ic-MRCI + QC, uc-MRCI and uc-MRCI + QC calculations, where +QC denotes inclusion of the renormalized Davidson correction [15, 27, 28]. The VRC-TST analysis depends on the location of pivot points for the rotational motions of the fragments. For large separations (>4 Å), the O_2 pivot point was placed at its center of mass, while for shorter separations pairs of pivot points displaced along the OO axis were considered. The displacement of these pivot points ranged from 0 to 1 Å. Distances ranging from 1.6 to 8 Å were considered for the H to pivot point separation. Convergence limits of 2 % were employed for the Monte Carlo integrations over the configurational integrals.

5 Results and discussion

MEPs for the title reaction obtained using uc-MRCI and ic-MRCI both with and without the Davidson correction and uc-AQCC and ic-AQCC are all presented in Fig. 1. The results are very similar to those presented in ref. [10]. A key question in this and other radical $+O_2$ reactions concerns the form of the long-range interaction potential (i.e., for separations ranging from about 2 to 3 Å). The results

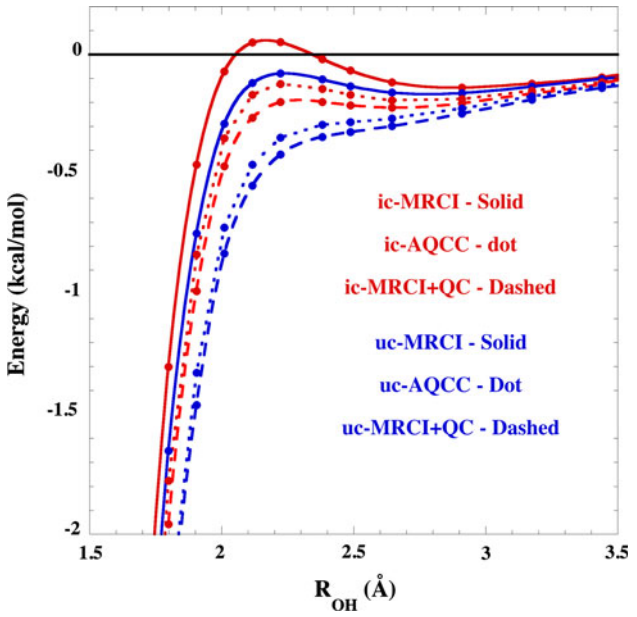

Fig. 1 Minimum energy path energies for the reaction $H + O_2 \rightarrow HO_2$ as a function of the OH bond length. The OO bond length and the HOO angle are optimized at the ic-CAS+1+2/aug-cc-pVTZ level

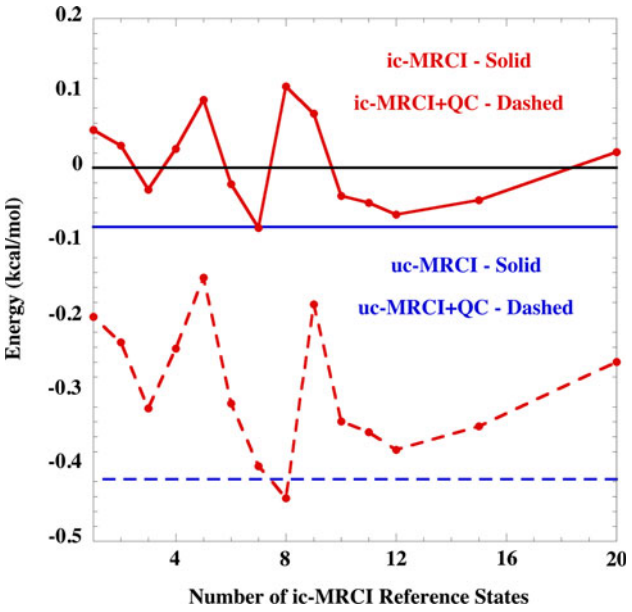

Fig. 2 Comparison of ic-MRCI and uc-MRCI interaction energies as a function of the number of reference states included in the ic-MRCI calculation. All calculations were performed at one intermediate point, $R_{OH} = 4.2$ au (2.22 Å), near the maximum on the ic-MRCI MEP shown in Fig. 1

shown in Fig. 1 illustrate that this long-range potential is very sensitive to the level of theory. The ic-CAS+1+2 calculations exhibit a small, positive barrier. The uc-CAS+1+2, ic-CAS+1+2+QC and ic-AQCC calculations all exhibit submerged barriers. Finally, the uc-CAS+1+2+QC and uc-AQCC calculations exhibit a potential that is monotonically attractive, i.e., with no PES barrier. Interestingly, the difference between the uc-MRCI and ic-MRCI calculations for the overall exothermicity of the reaction is very small, ~0.02 kcal/mol.

To check whether the differences between the ic-MRCI and uc-MRCI energies are primarily due to the contraction or to the interacting space restriction, additional calculations were carried out in which the number of reference states in the ic-MRCI calculations was varied. In principle if the number of references states is increased to equal the number of CSFs in the reference wave function, this should have the effect of fully uncontracting the ic-MRCI calculation within the interacting space. This is not practical for the 9-orbital active space used in the majority of calculations reported here. As a test, a limited number of calculations were performed with a smaller, 5-orbital, 7-electron active space consisting of the O_2 π and π* orbitals and the hydrogen 1s orbital. For these calculations, the reference wave function consists of 20 CSFs, and when all 20 reference states are included in the ic-MRCI calculation, the resulting interaction energy agrees to within 0.02 kcal/mol with the uc-MRCI calculation. This residual difference is presumably due to the differences in the expansion spaces discussed above. On a cautionary note, we find that the convergence of the ic-MRCI interaction energy as a function of increasing the number of reference states is highly non-monotonic. Although an increment in the number of reference states at a given molecular conformation results in a monotonic decrease in the total energy, the differences of these values can lead to either smaller or larger interaction energies and to non-systematic differences between these ic-MRCI and uc-MRCI energies. This is illustrated in Fig. 2 where the variation in the 9-active orbital ic-MRCI interaction energies (both with and without the Davidson correction) is shown as a function of the number of reference states (1–20) along with the corresponding uc-MRCI energy. Increasing the number of reference states to two or three is seen to result in small improvements in the agreement between the ic-MRCI and uc-MRCI interaction energies. However, other increments can result in significantly worse agreement.

The errors in the MRCI interaction potentials relative to the full-CI are presented in Fig. 3. Without the Davidson correction, the uc-MRCI calculations are in significantly better agreement with the full-CI calculations than are the ic-MRCI. The uc-MRCI calculations are in near perfect agreement with the full-CI for distances greater than 2.5 Å and then become slightly too attractive at shorter distances. The ic-MRCI calculations are not attractive enough in this region. However, inclusion of the Davidson correction changes this picture. With the Davidson correction, the uc-

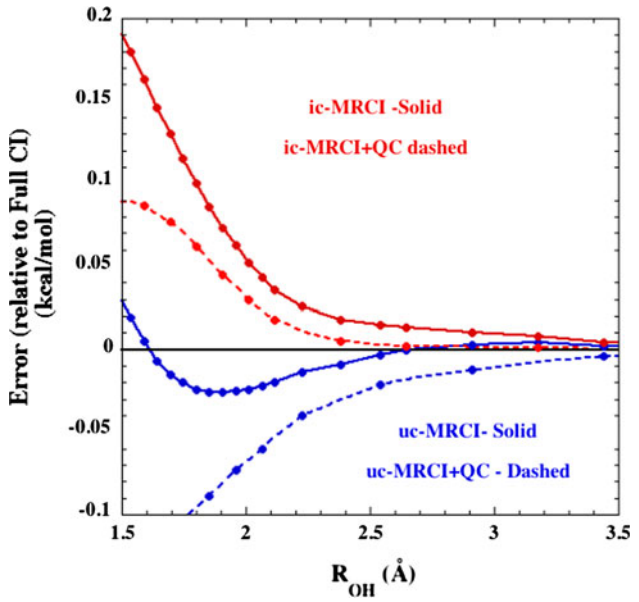

Fig. 3 Errors relative to full-CI in the uc-MRCI/VDZ and ic-MRCI/VDZ energies as a function of the OH bond length. The OO bond length is fixed at R_e, and the HOO bond angle is fixed at 115°

MRCI + QC calculations become too attractive at long range, while the ic-MRCI + QC are in near perfect agreement with full-CI at long range. At shorter distances, the magnitude of the error in the Davidson-corrected uc-MRCI + QC and ic-MRCI + QC calculations is comparable, with the uncontracted calculations being too attractive and the contracted calculation not attractive enough. It should be emphasized that these small-basis VDZ calculations capture only a small percentage of the correlation energy, and it is unclear to what extent these trends would persist with more flexible orbital basis sets. The full-CI total energies are listed in Table 1 of the Supplemental Information.

Contour plots of the uc-MRCI and ic-MRCI PESs for R_{OO} fixed at R_e are given in Fig. 4, and the difference between the two PESs is presented in Fig. 5. The plot shows that the differences between the uc-MRCI and ic-MRCI calculations are largest at H-center-of-mass distances of 1.5–2 Å. The differences also become larger near either the collinear or C_{2v} orientations. In this regard, it may be significant to note that conical intersections exist along both the collinear and C_{2v} approaches.

The results of the TST calculations of the rate are given in Fig. 6 along with experimental results from references [1, 4] and results employed in a recent modeling study of H_2/O_2 flame and ignition data [29]. The latter modeling study showed good agreement across a wide range of observables, including high-pressure flame data [30, 31], for which most other models were deficient. It employed the high-pressure limit obtained in the analysis of Troe [6],

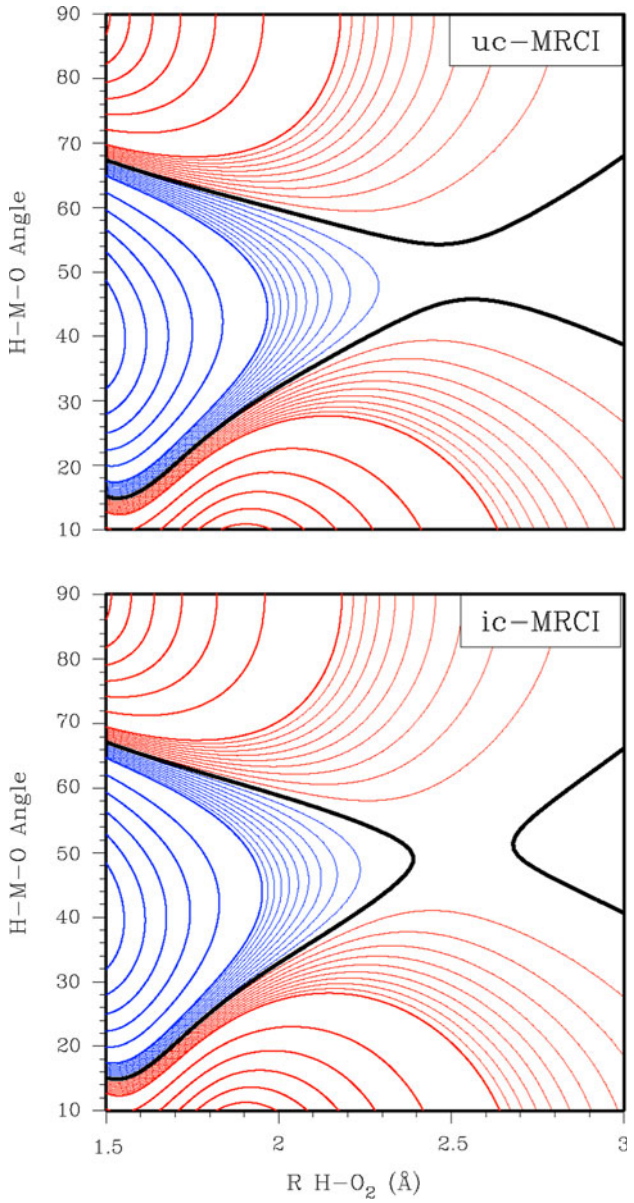

Fig. 4 Comparison of the uc-MRCI and ic-MRCI, CAS+1+2/aug-cc-pVTZ, H + O_2 interaction potentials for R_{OO} fixed at 1.21 Å. Blue contours represent regions lower in energy than the H + O_2 asymptote, while *red* contours represent energies higher than the asymptote, and the *black* contour corresponds to the energy of the asymptote. Contour increments for the heavy (*light*) contours are 5.0 kcal/mol (0.5 kcal/mol)

which in turn was based on the earlier potential energy surface study of Harding et al. [5]. At room temperature, the uc-MRCI-based calculations give rates that are ~30 % larger than the ic-MRCI-based calculations. Inclusion of the Davidson correction increases this difference to ~50 %. At the highest temperatures, the uc-MRCI and ic-MRCI results differ by only 5–10 %. The best agreement between theory and experiment comes from the Davidson-corrected uc-MRCI calculations although both of the

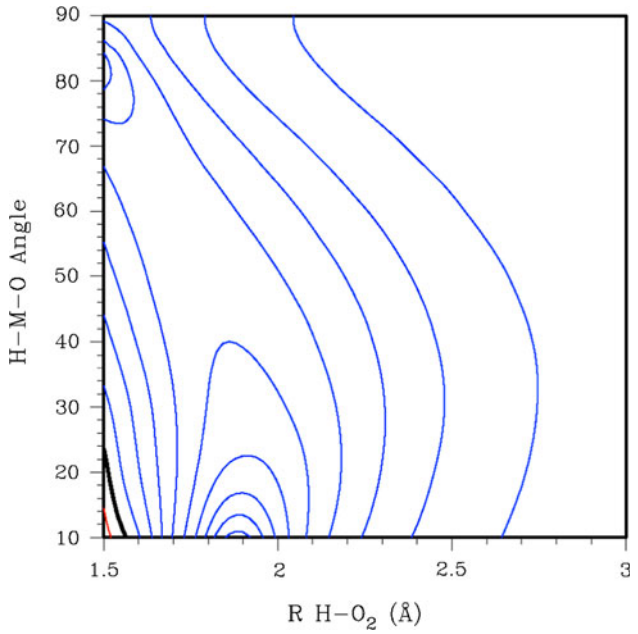

Fig. 5 The difference between the uc-MRCI and ic-MRCI CAS+1+2/aug-cc-pVTZ, $H + O_2$ interaction potentials for R_{OO} fixed at 1.21 Å. *Blue* contours represent regions where the uc-MRCI potential is more attractive (relative to the $H + O_2$ asymptote) than the ic-MRCI potential, while *red* contours represent regions where the ic-MRCI potential is more attractive. Contour increments for the heavy contours are 0.1 kcal/mol

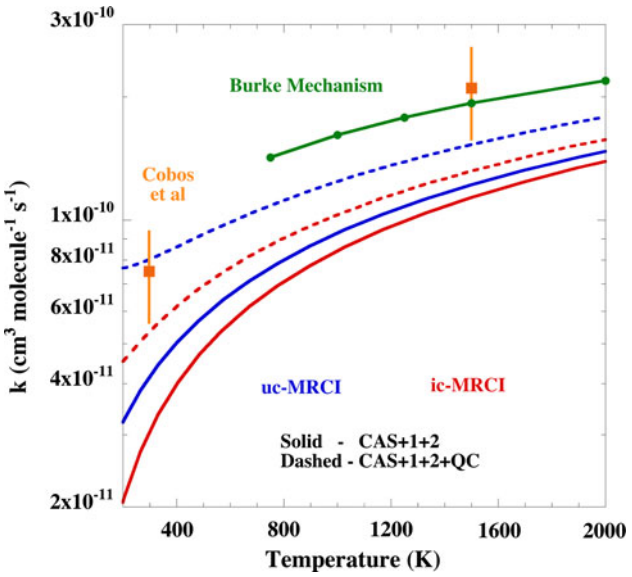

Fig. 6 Results of TST calculations on the high-pressure-limit rate for $H + O_2 \rightarrow HO_2$. The results using the uc-MRCI surfaces are shown in *blue* and the ic-MRCI in *red*. *Dashed lines* use PESs that include a Davidson correction. The *orange symbols* are experimental results [1, 4], and the *green line* is a result derived from a recent modeling study [29]

Davidson-corrected results are in reasonably good agreement with the experiment, given the uncertainty in the experimental data.

6 Conclusions

It is demonstrated that ic-MRCI calculations introduce small, but kinetically significant errors in interaction potentials relative to the corresponding uc-MRCI calculations. For the $H + O_2$ addition reaction, these errors are largest in the vicinity of the dynamical bottleneck. As dynamical bottlenecks often occur in regions where the character of the electronic wave function is changing rapidly (such as near-avoided crossings) and the wave function flexibility is critical, we expect this conclusion to be fairly general.

It is important to note that there is a significant difference in the computational cost of ic-MRCI and uc-MRCI calculations. For the CAS + 1 + 2/aug-cc-pVTZ calculations reported here, an uc-MRCI calculation requires approximately 40–50 times more computer time than the corresponding ic-MRCI calculation. This means that the use of the ic-MRCI approximation enables calculations with larger basis sets and active spaces than is currently feasible with uc-MRCI. When very high accuracy is needed, a hybrid approach might be most efficient in which the contraction error is evaluated with a relatively modest basis set and then applied as a correction to a larger basis set ic-MRCI interaction potential.

Acknowledgments This work was supported by the US Department of Energy, Office of Basic Energy Sciences, Division of Chemical Sciences, Geosciences, and Biosciences, under Contract Numbers DE-AC02-06CH11357. HL was also supported by the National Science Foundation under Project No. CHE-1213263 and by the Robert A.Welch Foundation under Grant No. D-0005.

References

1. Cobos CJ, Hippler H, Troe J (1985) J Phys Chem 89:342
2. Bates RW, Golden DM, Hanson RK, Bowman CT (2001) Phys Chem Chem Phys 3:2337
3. Hahn J, Krasnoperov L, Luther K, Troe J (2004) Phys Chem Chem Phys 6:1997
4. Cobos CJ, Troe J (1985) J Chem Phys 83:1010
5. Harding LB, Troe J, Ushakov VG (2000) Phys Chem Chem Phys 2:631
6. Troe J (2000) Proc Combust Inst 28:1463
7. Marques JMC, Varandas AJC (2001) Phys Chem Chem Phys 3:505
8. Harding LB, Troe J, Ushakov VG (2001) Phys Chem Chem Phys 3:2630
9. Lin SY, Rackham EJ, Guo H (2006) J Phys Chem A 110:1534
10. Sellevag SR, Georgievskii Y, Miller JA (2008) J Phys Chem 112:5085
11. Xu C, Xie D, Zhang DG, Lin SY, Guo H (2005) J Chem Phys 122:244035

12. Lischka H, Müller T, Szalay PG, Shavitt I, Pitzer RM, Shepard R (2011) WIREs Comput Mol Sci 1:191
13. MOLPRO, version 2010.1, a package of ab initio programs, Werner H-J, Knowles PJ, Manby FR, Schütz M, Celani P, Knizia G, Korona T, Lindh R, Mitrushenkov A, Rauhut G, Adler TB, Amos RD, Bernhardsson A, Berning A, Cooper DL, Deegan MJO, Dobbyn AJ, Eckert F, Goll E, Hampel C, Hesselmann A, Hetzer G, Hrenar T, Jansen G, Köppl C, Liu Y, Lloyd AW, Mata RA, May AJ, McNicholas SJ, Meyer W, Mura ME, Nicklass A, Palmieri P, Pflüger K, Pitzer RM, Reiher M, Shiozaka T, Stoll H, Stone AJ, Tarroni R, Thorsteinsson T, Wang M, Wolf A, see http://www.molpro.net
14. McLean AD, Liu B (1973) J Chem Phys 58:1066
15. Szalay PG, Mueller T, Gidofalvi G, Lischka H, Shepard R (2012) Chem Rev 112:108
16. Meyer, W (1977) In: Methods of electronic structure theory. Schaefer III HF (ed), Plenum: New York, pp 413–446
17. Werner H-J, Reinsch E-A (1982) J. Chem Phys 76:3144
18. Knowles PJ, Handy NC (1984) Chem Phys Lett 111:315
19. Knowles PJ, Handy NC (1989) Comp Phys Commun 54:75
20. Werner H-J, Knowles P (1988) J Chem Phys 89:5803
21. Knowles P, Werner H-J (1988) Chem Phys Lett 145:514
22. Kendall RA, Dunning TH Jr, Harrison RJ (1992) J Chem Phys 96:6796
23. Szalay PG, Bartlett RJ (1993) Chem Phys Lett 143:413
24. Dunning TH Jr (1989) J Chem Phys 90:1007
25. Klippenstein SJ (1992) J Chem Phys 96:367
26. Georgievskii Y, Klippenstein SJ (2003) J Phys Chem A 107:9776
27. Langhoff SR, Davidson ER (1974) Int J Quantum Chem 8:61
28. Bruckner KA (1955) Phys Rev 100:36
29. Burke MP, Chaos M, Ju Y, Dryer FL, Klippenstein SJ (2012) Int J Chem Kinet 44:444
30. Burke MP, Chaos M, Dryer FL, Ju Y (2010) Combust Flame 157:618
31. Burke MP, Dryer FL, Ju Y (2010) Proc Combust Inst 33:905